

Krylov complexity and gluon cascades in the high energy limit

Paweł Caputa^{1,2,*} and Krzysztof Kutak^{3,†}

¹*Faculty of Physics, University of Warsaw, Pasteura 5, 02-093 Warsaw, Poland*

²*Yukawa Institute for Theoretical Physics, Kyoto University,
Kitashirakawa Oiwakecho, Sakyo-ku, Kyoto 606-8502, Japan*

³*Institute of Nuclear Physics, Polish Academy of Sciences,
ul. Radzikowskiego 152, 31-342, Kraków, Poland*

(Dated: April 12, 2024)

We point out an interesting connection between the mathematical framework of the Krylov basis used for quantifying quantum complexity and entanglement entropy in high-energy QCD. In particular, we observe that the cascade equation of the dipole model is equivalent to the $SL(2, R)$ Schrodinger equation in the Krylov basis. Consequently, the Krylov complexity corresponds to the average distribution of partons and Krylov entropy matches entanglement entropy computations of [1]. Our work not only brings new tools for exploring quantum information and complexity in QCD but also gives hope for experimental tests of some of the recent, physical probes of quantum complexity.

Keywords: Complexity, Entanglement entropy, QCD

Introduction – Recently, the tools of quantum information (QI), such as entanglement or complexity, provide a new perspective on high-energy physics. This proves particularly fruitful in understanding quantum black holes in the AdS/CFT correspondence [2] (see e.g. [3]). Moreover, precise measures of quantum complexity are also believed to be crucial for understanding black hole interiors [4, 5]. These exciting developments motivated a new paradigm of exploring quantum systems from the angle of entanglement and complexity. In fact, in a series of papers [1, 6–22] authors argued that understanding entanglement in QCD may offer new insights into gluon dominated structure and properties of highly energetic hadrons. This was supported by the computation of entanglement entropy in electron-proton Deep Inelastic Scattering (DIS) process [1] that is based on the following logic. The proton is an eigenstate of the QCD Hamiltonian (a pure state), however, a measurement of its partonic content at some resolution scale introduces a bi-partition between resolved and unresolved parts that are entangled in an intricate way. This entanglement can be quantified by the von Neumann entropy

$$S_A = -\text{Tr}(\rho_A \log \rho_A) = -\sum_n p_n \ln p_n, \quad (1)$$

where $\rho_A = \text{Tr}_B(\rho_{AB})$ is the reduced density matrix of the resolved part A (B is its complement). The eigenvalues p_n are interpreted as probabilities of a state with definite number (n) of partons/dipoles. More importantly, [1] conjectured that this entanglement entropy is directly related to the hadronic entropy calculated using Gibbs formula after counting the

hadrons measured in the collider experiment. The motivation for this conjecture come from parton-hadron duality [23] where hadrons can be directly linked to partons which fragment and hadronize. Following this proposal, the measurement of hadronic entropy in DIS was performed [24] and appears consistent with the theoretical prediction [25–27]. Further evidence for the general picture of proton being the maximally entangled state came from studies of proton-proton collisions [28] and diffractive DIS [29] where the hadronic entropy has been successfully described.

In this work, we shed new light on this story by pointing to its mathematical equivalence with the Krylov space approach to quantum complexity [30–32]. Intuitively, it has been observed that dynamics of complexity and growth of quantum operators are well captured by epidemic/cascade models [33, 34] and parton evolution equations that we will consider are examples thereof. After making the connection precise, we will exploit it to bring new tools such as e.g. the capacity of entanglement, K-variance or continuum limits to the QCD discussions and probe the saturation effects.

Dipole cascade model – In this section we review the main findings of [1]. In QCD at high energies the convenient degrees of freedom of proton are color dipoles and quadrupoles [35–37]. The later, in a large number of color approximation, can be expressed as dipoles that represent a pair of highly energetic quarks or gluons. The usefulness of this representation comes from the fact that, at high energies, dipole’s size is fixed during interaction time and the S -matrix of the interaction is diagonal with respect to the transverse dipole size [36]. In [1, 13, 16], authors considered two scenarios: the 3+1 D Mueller’s picture (see [36] for review) [38] as well as it’s 1+1 D reduction. Here we focus on the 1+1 D case that is exactly solvable and, in the low x regime (explained below), approximates the Balitski, Fadin, Kuraev, Lipatov (BFKL) growth of gluon density

* pawel.caputa@fuw.edu.pl

† krzysztof.kutak@ifj.edu.pl

[39–42].

The probability $p_n(Y)$ of finding a state with n dipoles at rapidity Y (playing the role of the evolution time) obeys the equation [38, 43]

$$\partial_Y p_n(Y) = -\lambda n p_n(Y) + \lambda(n-1) p_{n-1}(Y), \quad (2)$$

where parameter λ characterizes the speed of the evolution. The first term in (2) describes the decrease in the probability due to the splitting into $(n+1)$ dipoles, while the second one – the growth due to the splitting of $(n-1)$ dipoles into n dipoles. The solutions of (2) are given by

$$p_n(Y) = e^{-\lambda Y} (1 - e^{-\lambda Y})^{n-1}, \quad (3)$$

and we plot some of them on fig. 1. At large rapidities, the probabilities tend to the same value which is interpreted as a state of maximal entanglement [1, 29]. We used $\lambda = 0.4$ which via formula $\lambda = 4\bar{\alpha}_s \ln 2$ can be related to the QCD coupling constant $\alpha_s = 0.15$, $\bar{\alpha}_s = N_c \alpha_s / \pi$, where $N_c = 3$ is a number of colors. The larger value of the coupling constant leads to faster evolution but essentially the features of the solutions are unchanged. The entropy (1) associated with system of dipoles is given by [1]

$$S = \lambda Y + (1 - e^{-\lambda Y}) \cdot \log(1 - e^{-\lambda Y}), \quad (4)$$

while the average number of dipoles grows exponentially with rapidity

$$\langle n \rangle = \sum_{n=1}^{\infty} n p_n(Y) = e^{\lambda Y}. \quad (5)$$

The equation above where $Y = \ln 1/x$ with Bjorken x - longitudinal momentum fraction of proton as carried by parton, is a model for BFKL momentum density of partons and it features the growth of partons (mainly gluons) with increasing rapidity. Taking the high energy

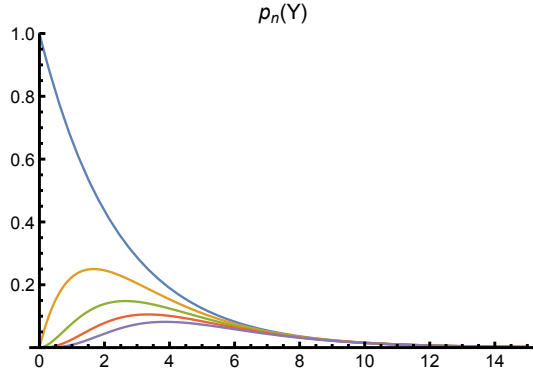


FIG. 1. Solutions of the equation ((2)) for p_n with n from 1 (the top blue line) to 5 (the purple line at the bottom) for $\alpha_s = 0.15$.

limit of eq. (4) and combining it with eq. (5) one gets the relation between entanglement and parton distribution ($g(x)$ - denoting the number of gluons at a given x) [1]

$$S \simeq \lambda Y = \ln \langle n \rangle \simeq \ln x g(x). \quad (6)$$

In the above the parton momentum density has been represented by gluons. The generalization accounting for quarks and charge factor can be found in [25].

Let us now momentarily switch to, a seemingly distant and unrelated corner of the high-energy theory, the Krylov complexity.

Krylov Complexity – Complexity is usually quantified using a circuit model where the circuit that performs a certain task is assembled from some universal set of gates. Task's complexity is defined as the minimal number of gates used to construct the circuit that accomplishes it [44]. Despite this simple intuition, quantifying complexity precisely in quantum systems, especially in quantum field theories, is very difficult. Nevertheless, a new physical measure of complexity of time evolution, defined as a spread in Hilbert space, has been recently developed at the interplay between many-body and high-energy physics. It started from the observation that epidemic models capture very well the growth of operators and evolution of complexity in holography [33, 34]. This was sharpened using the Krylov basis [30] and extended to a definition of state complexity in [32] (see also e.g. [45–51]). The key point is to expand the state or the operator in the minimal basis that supports its unitary evolution (the so-called Krylov basis). For concreteness, we review it for the state $|\Psi(t)\rangle$ that solves the Schrodinger equation with a general time-independent Hamiltonian H

$$|\Psi(t)\rangle = e^{-iHt} |\Psi_0\rangle = \sum_{n=0} \psi_n(t) |K_n\rangle. \quad (7)$$

The Krylov basis $|K_n\rangle$ is constructed by the iterative Gram-Schmidt procedure (the Lanczos algorithm [52]) applied to the Krylov subspace that consists of the initial state $|\Psi_0\rangle \equiv |K_0\rangle$ and all the powers of the Hamiltonian acting on it $H^n |\Psi_0\rangle$. The Lanczos algorithm produces a basis in which the Hamiltonian is tri-diagonal

$$H |K_n\rangle = a_n |K_n\rangle + b_n |K_{n-1}\rangle + b_{n+1} |K_{n+1}\rangle, \quad (8)$$

with a_n and b_n , called Lanczos coefficients, obtained in the iterative procedure. Consequently, the amplitudes $\psi_n(t)$ in (7) satisfy the Schrodinger equation

$$i\partial_t \psi_n(t) = a_n \psi_n(t) + b_{n+1} \psi_{n+1}(t) + b_n \psi_{n-1}(t). \quad (9)$$

Effectively, this approach maps the evolution to a one-dimensional chain with sites labeled by the index n of the Krylov basis vectors, and encodes dynamics into the probability distribution $p_n(t) \equiv |\psi_n(t)|^2$. This also brings us to the key concept of the Krylov complexity (K-complexity for short) defined as the average position

n on the chain

$$\mathcal{C}_K(t) = \langle n \rangle = \sum_n n p_n(t). \quad (10)$$

Of course, there is more information about the dynamics that is hidden in $p_n(t)$ than just in $\langle n \rangle$ and we often employ additional QI tools to probe it. The first one is the Shannon entropy measuring the information content of the distribution (dubbed the K-entropy [53])

$$S_K(t) = - \sum_n p_n(t) \log p_n(t). \quad (11)$$

Moreover, with K-variance we can quantify the fluctuations around the average position $\langle n \rangle$ [47]

$$\delta_K^2 = \frac{\langle n^2 \rangle - \langle n \rangle^2}{\langle n \rangle^2}. \quad (12)$$

In addition, from the m -th Renyi entropy

$$S_K^{(m)} = \frac{1}{1-m} \log \left(\sum_n p_n^m(t) \right), \quad (13)$$

we can define the analog of the heat capacity, the Capacity of Entanglement [54–56]

$$C_E = \lim_{m \rightarrow 1} m^2 \partial_m^2 [(1-m) S_K^{(m)}]. \quad (14)$$

The last quantity that we will consider is the purity defined as

$$\gamma_K = \sum_n p_n^2(t). \quad (15)$$

We will employ these tools to dipole cascades after we make a precise connection below.

Most importantly, equation (9) admits a class of analytic solutions with $a_n = 0$ and $b_n = \alpha n$ for some constant α (see Appendix A) given by

$$\psi_n(t) = (-i)^n \frac{\tanh^n(\alpha t)}{\cosh(\alpha t)}. \quad (16)$$

They were first derived in [30, 57] for the Sachdev-Ye-Kitaev (SYK) model [58, 59] and later explained using the dynamical $SL(2, \mathbb{R})$ symmetry in [31]. Interestingly, we can associate them with (7) evolved by the boost-type Hamiltonian

$$|\psi(t)\rangle = e^{-i\alpha(L_1 + L_{-1})t} |0\rangle \otimes |0\rangle, \quad (17)$$

where $L_{\pm 1}$ are the $SL(2, \mathbb{R})$ generators and $\psi_n(t)$ follow from the Baker–Campbell–Hausdorff relation for this Lie algebra. If we express them in the two-mode representation (see Appendix A) they are nothing but the Schmidt coefficients in this two-mode decomposition. The K-complexity for this solution grows exponentially

with time

$$\mathcal{C}_K(t) = \sum_{n=0}^{\infty} n |\psi_n(t)|^2 = \sinh^2(\alpha t), \quad (18)$$

while the K-entropy (11) (see also [60])

$$S_K(t) = 2 \log(\cosh(\alpha t)) - 2 \log(\tanh(\alpha t)) \sinh^2(\alpha t), \quad (19)$$

increases linearly for late times leading to the relation $\mathcal{C}_K(t) \sim \exp(S_K(t))$.

We conclude this part with an observation [30] that, from the exponential growth of $\mathcal{C}_K(t)$ at late times, we can define a Lyapunov exponent $\lambda_K = 2\alpha$. This growth in time is in fact correlated with the asymptotic growth of the Lanczos coefficients b_n with n that was conjectured to be at most linear

$$b_n \sim \alpha n + \kappa, \quad (20)$$

where α and κ are system dependent constants. For example, in the SYK model this bound is saturated and the Krylov-Lyapunov exponent coincides with the maximal chaos bound [61] from the Out-of-Time-Ordered correlators $\lambda_K = \lambda_{OTOC} = 2\pi/\beta$ where β is the inverse temperature $\beta = 1/T$ of the system.

The Connection – In this section we present the main results of our work. First, we observe that (9) implies an equation for the probabilities $p_n(t)$ (in complete analogy with the usual Schrodinger and continuity equations). More precisely, we can show that $p_n(t) = |\psi_n(t)|^2$ associated with solution (16) satisfy the cascade equation

$$\partial_Y p_n(Y) = \alpha n p_{n-1}(Y) - \alpha(n+1) p_n(Y), \quad (21)$$

where we introduced a “rapidity” variable Y related to the time t via

$$\tanh^2(\alpha t) = 1 - e^{-\alpha Y}. \quad (22)$$

This is almost the same as (2), and the only difference is the range of index n . Namely, in the QCD model n is the number of dipoles $n \in (1, \infty)$ and in the Krylov basis we have $n \in (0, \infty)$. Indeed, shifting the index $n \rightarrow n+1$ we verify that the $SL(2, \mathbb{R})$ solution expressed in terms of Y satisfies the cascade equation (2) after identifying α with λ . Consequently, the average dipole number $\langle n \rangle$ maps to the Krylov complexity (more precisely $\mathcal{C}_K + 1$)¹. Given the above and using eq. (5) we may write the relation between the K-complexity (in the cascade model) and

¹In [16] the summation index n is shifted so that in the case the relation to Krylov complexity does not need shift. The arbitrariness is related to choice of initial condition and is not relevant at high energy limit.

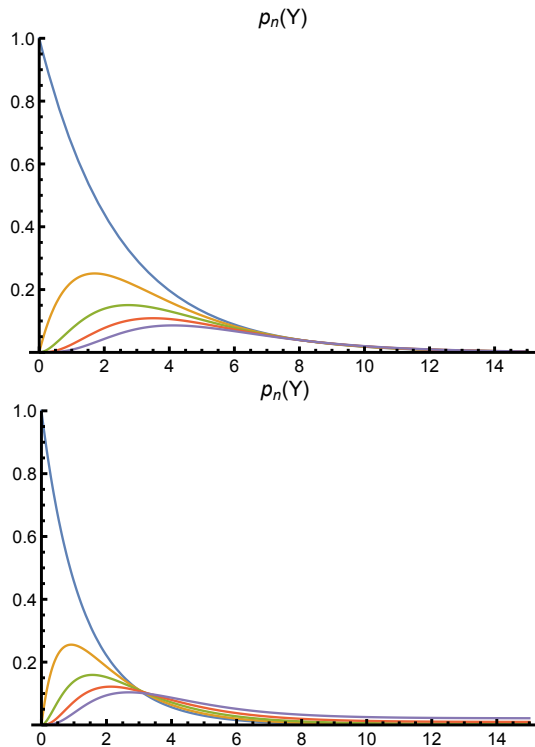


FIG. 2. Solutions of the equation ((24)) for p_n from 1 (the top blue line) to 5 (the bottom purple line). Upper plot: $\alpha_s = 0.15$. Lower plot: $\alpha_s = 0.3$.

patron distribution

$$\mathcal{C}_K = xg(x). \quad (23)$$

We note also that the entanglement entropy (4) is the counterpart of the K-entropy. These connections are one of our main results².

Let us finally point that the coefficients in the cascade equation, eq. (2), satisfy the bound (20) (choosing $\alpha = \lambda$ and $\kappa = 0$). Whether this reflects any "chaotic" or scrambling properties of QCD, i.e., $\lambda = 4\bar{\alpha}_s \ln 2$ plays the role of the Lyapunov exponent, is beyond the scope of this work, but it would be fascinating to explore these questions, given the bulk of developments following [61]. After explaining the relation between these two developments, in the next sections we will study a generalised dipole evolution equation that takes into account saturation effects and probe it with QI tools from the Krylov approach. Understanding possible mechanisms behind both, the saturation of parton density and the saturation of complexity are very important and we will explore them in this tractable QCD scenario.

Dipole cascade with recombinations – In QCD at high energies, there is an expectation that once the density of partons is high enough, gluons not only split but also recombine. The recombination changes the exponential growth of the number of gluons (with rapidity) and leads to saturation [35, 62] (see also [36, 63] for review). While there are hints for saturation of gluons [36, 64], the strong evidence is still lacking and search for saturation is the subject of forthcoming programs, both at Electron Ion Collider [65] and Large Hadron Collider [66, 67]. Evolution equations that account for gluon saturation are nonlinear generalizations [68–73] of the BFKL equation. The 1+1 dipole model can also be generalised to account for recombination that leads to saturation. The generalised evolution equation reads [74, 75]

$$\begin{aligned} \partial_Y p_n(Y) = & -\lambda n p_n(Y) + \lambda(n-1)p_{n-1}(Y) \\ & + \beta n(n+1)p_{n+1}(Y) - \beta n(n-1)p_n(Y), \end{aligned} \quad (24)$$

where $\beta = \lambda\alpha_s^2$. Clearly, the first two terms are the same as in (2) while the last two account for dipole recombination. The proportionality of the recombination terms with α_s^2 indicates that they are relevant at large values of rapidity when the smallness of the coupling constant is compensated by the large number of dipoles. This equation was solved analytically in the approximation of large Y in [76] but, in order to test our new QI tools in this context, we just solve it numerically with initial conditions $p_1(0) = 1$ and $p_n(0) = 0$ for $n > 1$ (see also Appendix B for solutions in the continuum limit). The resulting probabilities are plotted on fig. 2 and the curves are similar to those on fig. 1. Nevertheless, the behavior drastically changes as we increase the value of the coupling α_s . In this regime the term responsible for dipole recombination starts to play an important role already at lower rapidities. It also leads to a scenario where at asymptotic rapidities the probability with a large number of dipoles dominates and is actually increasing as rapidity increases.

QI tools for dipole cascades – Finally, we apply the QI tools from the Krylov framework to the dipole cascade model both with and without fluctuations. More precisely, we evaluate the K-complexity (10), the K-entropy (11) and the K-variance (12). Moreover, we evaluate the capacity of entanglement (14), that contains information about the width of the eigenvalue distribution of the reduced density matrix [54] and the purity (15), that is strictly 1 for pure states and departures from this value as system becomes mixed. First, on fig. 3, we plot the QI measures that characterize the dipole cascade eq. (2) using the exact solution of [38]. We confirm earlier results that the entropy grows linearly with Y reaching maximally entangled state [1] at large rapidities. This is also supported by the value of purity going to zero. The rate of the growth of entropy is given by λ and complexity grows exponentially. We also find that capacity of entanglement measuring entanglement

²We should also point out that (3) appeared in the context of the operator growth in SYK [57] but it had Y replaced by t and there was no relation with the Krylov approach.

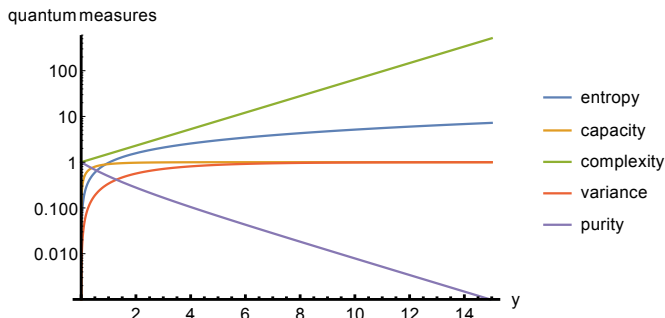


FIG. 3. Quantum measures applied to solutions of eq. ((2)). The plot is for $\alpha_s = 0.15$.

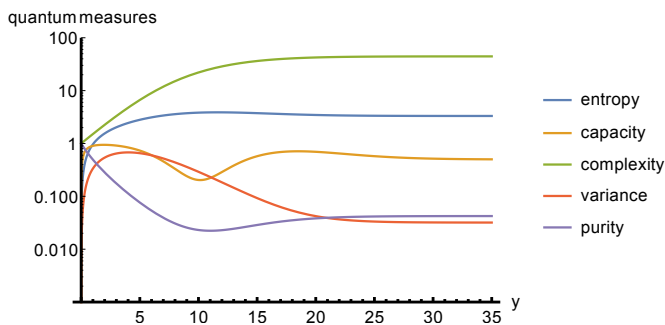


FIG. 4. Quantum measures applied to solutions of eq. ((24)). Plot for $\alpha_s = 0.15$.

spreading saturates at unity.

Next we plot the same measures for the solutions of the dipole model that accounts for recombinations. The complexity initially grows but at large rapidities saturates³. From the QCD perspective, this behaviour confirms an expected feature of the interplay between the splitting and recombination terms in the eq. (24). The entropy however develops maximum as it was observed in [76] and saturates at larger rapidities. We note that such behaviour is consistent with gluon densities obtained with QCD evolution equations that take into account transverse degrees of freedom [26]. This is also consistent with evolution of capacity of entanglement which has the minimum (see Appendix C for plot in the linear scale). Interestingly the system does not reach a state where purity drops to zero indicating departure from the maximally entangled state. Overall, we interpret this behaviour as indication of “classicalization” [77] i.e. the emergence of scale in the system. In our case this is the value of rapidity for which the capacity has minimum and complexity saturates. This is also consistent with results from fig (5) where the negativity of system with saturation is lower.

Conclusions and discussion – In conclusion, we established a connection between the framework of the

evolution of states with dynamical $SL(2, R)$ symmetry in Krylov basis and the evolution of dipoles in 1+1 dimensional Mueller dipole cascade model. This new link allowed us relate the K-complexity to the number of dipoles and K-entropy to entanglement entropy of dipoles in DIS discussed in [1]. The results using the simple dipole model in 1+1 D have a chance to hold more generally. In particular, the dipole model in 3+1 D has formally the same structure as the 1+1 D model. This suggests that Krylov space methods should be applicable as well and the relation of quantum complexity to the gluon density can be generalised more broadly.

We also imported some of the new, useful QI tools to explore more fine-grained properties of the dipole cascade models. The first of the model features linear growth of the entropy with rapidity [1, 22, 78] and exponential growth of complexity. While the second model shows the saturation of these measures. Interestingly, from the quantum complexity perspective, we usually think about the saturation of complexity as a consequence of the finite Hilbert space. However, in the QCD model saturation comes from the interplay between splitting and recombination of partons (both infinite dimensional). It will be very interesting to understand this mechanism from a more QI perspective, and we leave it as an important future problem.

We also analysed the variance, capacity and purity measures. The models with and without saturation predict very different behaviour of these new, potentially measurable quantities. Note that for example the evolution of capacity shows a characteristic minimum at the maximal value of the entropy. Therefore, it can potentially be a more sensitive probe of degree of parton’s entanglement to detect.

Last but not the least, we are certain that these QI tools will not only be useful for future analysis of entanglement structure governed by more realistic QCD evolution equations but may also be measurable under the same assumptions as the hadronic entropy.

Acknowledgements – We are grateful to Vijay Balasubramanian, Martin Hentschinski, Javier Magan, Dimitrios Patramanis and Douglas Stanford for discussions and comments. PC is supported by NAWA “Polish Returns 2019” PPN/PPO/2019/1/00010/U/0001 and NCN Sonata Bis 9 2019/34/E/ST2/00123 grants. PC would also like to thank the Isaac Newton Institute for Mathematical Sciences, Cambridge, for support and hospitality during the programme “Black Holes: bridges between number theory and holographic quantum information”, where work on this paper was undertaken and presented as well as KITP, UCSB for support during final stages of this project. KK acknowledges the European Union’s Horizon 2020 research and innovation programme under grant agreement No. 824093.

-
- [1] D. E. Kharzeev and E. M. Levin, *Phys. Rev. D* **95**, 114008 (2017), [arXiv:1702.03489 \[hep-ph\]](#).
- [2] J. M. Maldacena, *Adv. Theor. Math. Phys.* **2**, 231 (1998), [arXiv:hep-th/9711200](#).
- [3] A. Almheiri, T. Hartman, J. Maldacena, E. Shaghoulian, and A. Tajdini, (2020), [arXiv:2006.06872 \[hep-th\]](#).
- [4] L. Susskind, *Fortsch. Phys.* **64**, 24 (2016), [Addendum: *Fortsch. Phys.* **64**, 44–48 (2016)], [arXiv:1403.5695 \[hep-th\]](#).
- [5] A. R. Brown, D. A. Roberts, L. Susskind, B. Swingle, and Y. Zhao, *Phys. Rev. Lett.* **116**, 191301 (2016), [arXiv:1509.07876 \[hep-th\]](#).
- [6] K. Kutak, *Phys. Lett. B* **705**, 217 (2011), [arXiv:1103.3654 \[hep-ph\]](#).
- [7] R. Peschanski, *Phys. Rev. D* **87**, 034042 (2013), [arXiv:1211.6911 \[hep-ph\]](#).
- [8] A. Stoffers and I. Zahed, *Phys. Rev. D* **88**, 025038 (2013), [arXiv:1211.3077 \[nucl-th\]](#).
- [9] N. Armesto, F. Dominguez, A. Kovner, M. Lublinsky, and V. Skokov, *JHEP* **05**, 025 (2019), [arXiv:1901.08080 \[hep-ph\]](#).
- [10] A. Kovner, M. Lublinsky, and M. Serino, *Phys. Lett. B* **792**, 4 (2019), [arXiv:1806.01089 \[hep-ph\]](#).
- [11] A. Kovner, E. Levin, and M. Lublinsky, *JHEP* **05**, 019 (2022), [arXiv:2201.01551 \[hep-ph\]](#).
- [12] Y. Liu, M. A. Nowak, and I. Zahed, *Phys. Rev. D* **105**, 114027 (2022), [arXiv:2202.02612 \[hep-ph\]](#).
- [13] Y. Liu, M. A. Nowak, and I. Zahed, *Phys. Rev. D* **108**, 034017 (2023), [arXiv:2211.05169 \[hep-ph\]](#).
- [14] A. Dumitru and E. Kolbusz, *Phys. Rev. D* **105**, 074030 (2022), [arXiv:2202.01803 \[hep-ph\]](#).
- [15] D. E. Kharzeev, *Phil. Trans. A. Math. Phys. Eng. Sci.* **380**, 20210063 (2021), [arXiv:2108.08792 \[hep-ph\]](#).
- [16] Y. Liu, M. A. Nowak, and I. Zahed, *Phys. Rev. D* **105**, 114028 (2022), [arXiv:2203.00739 \[hep-ph\]](#).
- [17] Y. Liu, M. A. Nowak, and I. Zahed, *Phys. Rev. D* **108**, 094025 (2023), [arXiv:2301.06154 \[hep-ph\]](#).
- [18] Y. Liu, M. A. Nowak, and I. Zahed, *Phys. Rev. D* **107**, 054010 (2023), [arXiv:2205.06724 \[hep-ph\]](#).
- [19] Y. Liu, M. A. Nowak, and I. Zahed, (2023), [arXiv:2302.01380 \[hep-ph\]](#).
- [20] A. Dumitru and E. Kolbusz, *Phys. Rev. D* **108**, 034011 (2023), [arXiv:2303.07408 \[hep-ph\]](#).
- [21] G. Chachamis, M. Hentschinski, and A. Sabio Vera, (2023), [arXiv:2312.16743 \[hep-th\]](#).
- [22] K. Kutak, (2023), [arXiv:2310.18510 \[hep-ph\]](#).
- [23] Y. L. Dokshitzer, V. A. Khoze, S. I. Troian, and A. H. Mueller, *Rev. Mod. Phys.* **60**, 373 (1988).
- [24] V. Andreev *et al.* (H1), *Eur. Phys. J. C* **81**, 212 (2021), [arXiv:2011.01812 \[hep-ex\]](#).
- [25] M. Hentschinski and K. Kutak, *Eur. Phys. J. C* **82**, 111 (2022), [Erratum: *Eur. Phys. J. C* **83**, 1147 (2023)], [arXiv:2110.06156 \[hep-ph\]](#).
- [26] M. Hentschinski, K. Kutak, and R. Straka, *Eur. Phys. J. C* **82**, 1147 (2022), [arXiv:2207.09430 \[hep-ph\]](#).
- [27] W. Kou, X. Wang, and X. Chen, *Phys. Rev. D* **106**, 096027 (2022), [arXiv:2208.07521 \[hep-ph\]](#).
- [28] Z. Tu, D. E. Kharzeev, and T. Ullrich, *Phys. Rev. Lett.* **124**, 062001 (2020), [arXiv:1904.11974 \[hep-ph\]](#).
- [29] M. Hentschinski, D. E. Kharzeev, K. Kutak, and Z. Tu, *Phys. Rev. Lett.* **131**, 241901 (2023), [arXiv:2305.03069 \[hep-ph\]](#).
- [30] D. E. Parker, X. Cao, A. Avdoshkin, T. Scaffidi, and E. Altman, *Phys. Rev. X* **9**, 041017 (2019), [arXiv:1812.08657 \[cond-mat.stat-mech\]](#).
- [31] P. Caputa, J. M. Magan, and D. Patramanis, *Phys. Rev. Res.* **4**, 013041 (2022), [arXiv:2109.03824 \[hep-th\]](#).
- [32] V. Balasubramanian, P. Caputa, J. M. Magan, and Q. Wu, *Phys. Rev. D* **106**, 046007 (2022), [arXiv:2202.06957 \[hep-th\]](#).
- [33] L. Susskind and Y. Zhao, (2014), [arXiv:1408.2823 \[hep-th\]](#).
- [34] X.-L. Qi and A. Streicher, *JHEP* **08**, 012 (2019), [arXiv:1810.11958 \[hep-th\]](#).
- [35] A. H. Mueller and J.-w. Qiu, *Nucl. Phys. B* **268**, 427 (1986).
- [36] Y. V. Kovchegov and E. Levin, *Quantum Chromodynamics at High Energy*, Vol. 33 (Oxford University Press, 2013).
- [37] F. Dominguez, C. Marquet, A. M. Stasto, and B.-W. Xiao, *Phys. Rev. D* **87**, 034007 (2013), [arXiv:1210.1141 \[hep-ph\]](#).
- [38] A. H. Mueller, *Nucl. Phys. B* **437**, 107 (1995), [arXiv:hep-ph/9408245](#).
- [39] I. I. Balitsky and L. N. Lipatov, *Sov. J. Nucl. Phys.* **28**, 822 (1978).
- [40] E. A. Kuraev, L. N. Lipatov, and V. S. Fadin, *Sov. Phys. JETP* **45**, 199 (1977).
- [41] J. Kwiecinski, A. D. Martin, and A. M. Stasto, *Phys. Rev. D* **56**, 3991 (1997), [arXiv:hep-ph/9703445](#).
- [42] M. Hentschinski, A. Sabio Vera, and C. Salas, *Phys. Rev. D* **87**, 076005 (2013), [arXiv:1301.5283 \[hep-ph\]](#).
- [43] E. Levin and M. Lublinsky, *Nucl. Phys. A* **730**, 191 (2004), [arXiv:hep-ph/0308279](#).
- [44] C. E. Shannon, *The Bell System Technical Journal* **28**, 59 (1949).
- [45] E. Rabinovici, A. Sánchez-Garrido, R. Shir, and J. Sonner, *JHEP* **06**, 062 (2021), [arXiv:2009.01862 \[hep-th\]](#).
- [46] A. Dymarsky and M. Smolkin, *Phys. Rev. D* **104**, L081702 (2021), [arXiv:2104.09514 \[hep-th\]](#).
- [47] P. Caputa and S. Datta, *JHEP* **12**, 188 (2021), [Erratum: *JHEP* **09**, 113 (2022)], [arXiv:2110.10519 \[hep-th\]](#).
- [48] P. Caputa and S. Liu, *Phys. Rev. B* **106**, 195125 (2022), [arXiv:2205.05688 \[hep-th\]](#).
- [49] E. Rabinovici, A. Sánchez-Garrido, R. Shir, and J. Sonner, *JHEP* **08**, 213 (2023), [arXiv:2305.04355 \[hep-th\]](#).
- [50] S.-K. Jian, B. Swingle, and Z.-Y. Xian, *JHEP* **03**, 014 (2021), [arXiv:2008.12274 \[hep-th\]](#).
- [51] C. von Keyserlingk, T. Rakovszky, F. Pollmann, and S. Sondhi, *Phys. Rev. X* **8**, 021013 (2018), [arXiv:1705.08910 \[cond-mat.str-el\]](#).
- [52] V. S. Viswanath and G. Müller, *The Recursion Method: Application to Many-Body Dynamics* (Springer Berlin, Heidelberg, Germany, 1994).

³Note that the enormous rapidity range that we use is relevant for our theoretical study of the models. The phenomenologically relevant rapidity range is $Y < 7$.

- [53] J. L. F. Barbón, E. Rabinovici, R. Shir, and R. Sinha, *JHEP* **10**, 264 (2019), arXiv:1907.05393 [hep-th].
- [54] H. Yao and X.-L. Qi, *Physical Review Letters* **105** (2010), 10.1103/physrevlett.105.080501.
- [55] J. De Boer, J. Järvelä, and E. Keski-Vakkuri, *Phys. Rev. D* **99**, 066012 (2019), arXiv:1807.07357 [hep-th].
- [56] K. Kawabata, T. Nishioka, Y. Okuyama, and K. Watanabe, *JHEP* **05**, 062 (2021), arXiv:2102.02425 [hep-th].
- [57] D. A. Roberts, D. Stanford, and A. Streicher, *JHEP* **06**, 122 (2018), arXiv:1802.02633 [hep-th].
- [58] S. Sachdev and J. Ye, *Phys. Rev. Lett.* **70**, 3339 (1993), arXiv:cond-mat/9212030.
- [59] A. Kitaev, Talks at KITP, April 7, 2015 and May 27..
- [60] D. Patramanis, *PTEP* **2022**, 063A01 (2022), arXiv:2111.03424 [hep-th].
- [61] J. Maldacena, S. H. Shenker, and D. Stanford, *JHEP* **08**, 106 (2016), arXiv:1503.01409 [hep-th].
- [62] L. V. Gribov, E. M. Levin, and M. G. Ryskin, *Phys. Rept.* **100**, 1 (1983).
- [63] F. Gelis, E. Iancu, J. Jalilian-Marian, and R. Venugopalan, *Ann. Rev. Nucl. Part. Sci.* **60**, 463 (2010), arXiv:1002.0333 [hep-ph].
- [64] J. L. Albacete and C. Marquet, *Prog. Part. Nucl. Phys.* **76**, 1 (2014), arXiv:1401.4866 [hep-ph].
- [65] R. Abdul Khalek *et al.*, *Nucl. Phys. A* **1026**, 122447 (2022), arXiv:2103.05419 [physics.ins-det].
- [66] A. Morreale and F. Salazar, *Universe* **7**, 312 (2021), arXiv:2108.08254 [hep-ph].
- [67] A. van Hameren, H. Kakkad, P. Kotko, K. Kutak, and S. Sapeta, *Eur. Phys. J. C* **83**, 947 (2023), arXiv:2306.17513 [hep-ph].
- [68] Y. V. Kovchegov, *Phys. Rev. D* **60**, 034008 (1999), arXiv:hep-ph/9901281.
- [69] Y. V. Kovchegov, *Phys. Rev. D* **61**, 074018 (2000), arXiv:hep-ph/9905214.
- [70] I. Balitsky, *Nucl. Phys. B* **463**, 99 (1996), arXiv:hep-ph/9509348.
- [71] E. Iancu, A. Leonidov, and L. D. McLerran, *Phys. Lett. B* **510**, 133 (2001), arXiv:hep-ph/0102009.
- [72] J. Jalilian-Marian, A. Kovner, A. Leonidov, and H. Weigert, *Phys. Rev. D* **59**, 014014 (1998), arXiv:hep-ph/9706377.
- [73] J. Jalilian-Marian, A. Kovner, A. Leonidov, and H. Weigert, *Nucl. Phys. B* **504**, 415 (1997), arXiv:hep-ph/9701284.
- [74] A. I. Shoshi and B.-W. Xiao, *Phys. Rev. D* **73**, 094014 (2006), arXiv:hep-ph/0512206.
- [75] S. Bondarenko, L. Motyka, A. H. Mueller, A. I. Shoshi, and B. W. Xiao, *Eur. Phys. J. C* **50**, 593 (2007), arXiv:hep-ph/0609213.
- [76] Y. Hagiwara, Y. Hatta, B.-W. Xiao, and F. Yuan, *Phys. Rev. D* **97**, 094029 (2018), arXiv:1801.00087 [hep-ph].
- [77] G. Dvali and R. Venugopalan, *Phys. Rev. D* **105**, 056026 (2022), arXiv:2106.11989 [hep-th].
- [78] U. Gürsoy, D. E. Kharzeev, and J. F. Pedraza, (2023), arXiv:2306.16145 [hep-th].
- [79] G. Vidal and R. F. Werner, *Phys. Rev. A* **65**, 032314 (2002), arXiv:quant-ph/0102117.

Appendix A: General SL(2,R) solutions

In this appendix we provide a brief summary of the analytical solution (16) and use it to evaluate QI tools discussed in the main text.

A general class of analytical solutions to equation (9) can be obtained when

$$a_n = \gamma(n + h), \quad b_n = \alpha\sqrt{n(2h + n - 1)}. \quad (\text{A1})$$

for parameters γ and α that depend on the physical details of the initial state and evolving Hamiltonian. Parameter h corresponds to the conformal dimension of the operator that growth we consider. As described in [31], these Lanczos coefficients reflect the underlying dynamical SL(2,R) symmetry of the Krylov basis for a given physical problem.

In what follows, we focus on the case when $\gamma = 0$, for which the solution $\psi_n(t)$ yields the probabilities

$$p_n(t) = |\psi_n(t)|^2 = \frac{\Gamma(2h + n) \tanh^{2n}(\alpha t)}{n! \Gamma(2h) \cosh^{4h}(\alpha t)}. \quad (\text{A2})$$

It is useful to think about this example as a state

$$|\psi(t)\rangle = e^{i\alpha(a^\dagger b^\dagger + ab)t} |0\rangle \otimes |0\rangle, \quad (\text{A3})$$

where the operators in the exponent $L_{-1} = a^\dagger b^\dagger$ and $L_1 = ab$, are the raising and lowering operators of the SL(2,R) Lie algebra. The third generator $L_0 = \frac{1}{2}(a^\dagger a + b^\dagger b + 1)$ and $|0\rangle \otimes |0\rangle$ is its eigenstate $L_0 |h\rangle = k |k\rangle$ with $h = 1/2^4$. This is simply a special case of the coherent state of the SU(1,1) (SL(2,R)) algebra and we can expand it as

$$|\psi(t)\rangle = \sum_{n=0}^{\infty} \frac{\tanh^n(\alpha t)}{\cosh^{2h}(\alpha t)} \sqrt{\frac{\Gamma(2h + n)}{n! \Gamma(2h)}} |n\rangle \otimes |n\rangle. \quad (\text{A4})$$

We think about this state as a Schmidt decomposition in the product of two Hilbert spaces such that tracing out over one of them yields the density matrix

$$\rho(t) = \sum_{n=0}^{\infty} p_n(t) |n\rangle \langle n|. \quad (\text{A5})$$

It is useful to rewrite this probabilities in terms of the rapidity variable Y

$$p_n(Y) = \frac{\Gamma(2h + n)}{n! \Gamma(2h)} (e^{-\alpha Y})^{2h} (1 - e^{-\alpha Y})^n. \quad (\text{A6})$$

⁴general h can be obtained by acting with the same exponent (A3) on the initial state with $k = 2h - 1$ difference between the modes. These are the k -added or subtracted states in the quantum optics jargon.

This probability satisfies a cascade equation

$$\partial_Y p_n(Y) = \alpha(n+2h-1)p_{n-1}(Y) - \alpha(n+2h)p_n(Y), \quad (\text{A7})$$

and for $h = 1/2$ we recover our example (21).

One way to understand this equation is simply by analogy with the Schrodinger equation for the wave function and continuity equation for the probabilities. Indeed we can just write our Schrodinger equations for the Krylov wave function and for its complex conjugate, multiply them by the conjugate wave functions and add. The left hand side is the derivative of the probability $p_n(t)$ and the right side is a combination of different wave functions and their conjugate. We can check that our SL(2,R) solution have the property that the right hand side can be rewritten as equation above times overall function of t . Finally, changing variables to Y gets rid of this factor and yields the equation above.

Next, to present the analytical results for the QI measures, it is useful to parametrize our probability distribution by variable

$$z\bar{z} = 1 - e^{-\alpha Y} = \tanh^2(\alpha t), \quad (\text{A8})$$

such that

$$p_n = (1 - z\bar{z})(z\bar{z})^n. \quad (\text{A9})$$

Then we have all our quantities in terms of $z\bar{z}$ we have

$$C_K = \langle n \rangle = \frac{z\bar{z}}{1 - z\bar{z}}, \quad (\text{A10})$$

while the K-entropy is given by

$$S_K = \log \left(\frac{z\bar{z}}{1 - z\bar{z}} \right) - \frac{\log(z\bar{z})}{1 - z\bar{z}}. \quad (\text{A11})$$

Clearly, have the relation

$$S_K = \log \langle n \rangle - \frac{\log(z\bar{z})}{1 - z\bar{z}}, \quad (\text{A12})$$

that for late times, as $z\bar{z} \rightarrow 1$, relates S_K and K-complexity $\langle n \rangle$. The variance is simply given by

$$\delta_K^2 = (z\bar{z})^{-1}. \quad (\text{A13})$$

Moreover, the Renyi entropies

$$S^{(m)} = \frac{1}{1-m} \log \left(\frac{(1 - z\bar{z})^m}{1 - (z\bar{z})^m} \right), \quad (\text{A14})$$

give rise to the capacity of entanglement

$$C_E = \frac{z\bar{z} \log(z\bar{z})^2}{(1 - z\bar{z})^2}. \quad (\text{A15})$$

Finally, we can also derive the purity as

$$\gamma_K = \frac{1 - z\bar{z}}{1 + z\bar{z}}. \quad (\text{A16})$$

Plugging $z\bar{z}$ from (A8) reproduces our results from the main text.

Appendix B: The continuum limit

It is often useful to consider the continuum limit of the discrete chain equation [53] and we repeat this procedure for the general model with saturation. Namely starting from (24), we can write it as

$$\partial_Y p_n = b_{n-1}p_{n-1} - b_n p_n + c_{n+1}p_{n+1} - c_n p_n, \quad (\text{B1})$$

where in our explicit equation we have $b_n = \lambda n$ and $c_n = \beta n(n-1)$, but we keep them general for the moment.

Next we define the continuous variable $x \equiv \epsilon n$, such that

$$p_n(Y) \equiv p(x, Y), \quad p_{n\pm 1} = p(x \pm \epsilon, Y). \quad (\text{B2})$$

Moreover, we write

$$\epsilon b_n \equiv v(x), \quad \epsilon c_n \equiv w(x), \quad (\text{B3})$$

as well as

$$\epsilon b_{n-1} = v(x - \epsilon), \quad \epsilon c_{n+1} = w(x + \epsilon). \quad (\text{B4})$$

After expanding for $\epsilon \simeq 0$ we derive the continuum equation

$$\partial_Y p(x, Y) + \partial_x j(x, Y) = 0, \quad (\text{B5})$$

where

$$j(x, Y) = (w(x) - v(x)) p(x, Y). \quad (\text{B6})$$

For $\beta = 0$ and $v(x) = \lambda x$ we reproduce [53], but the generalised equation is responsible for the effective $\tilde{v}(x) = w(x) - v(x)$. For example, we can take the initial Gaussian profile

$$p(x, 0) = \sqrt{\frac{2}{\pi}} \frac{1}{\sigma} e^{-\frac{x^2}{2\sigma^2}}, \quad (\text{B7})$$

such that, if $v(x) = \lambda x$ and $\beta = 0$, the solution becomes

$$p(x, Y) = \sqrt{\frac{2}{\pi}} \frac{1}{\sigma} \exp \left(-\lambda Y - e^{-2\lambda Y} \frac{x^2}{2\sigma^2} \right). \quad (\text{B8})$$

This gives the exponential growth of complexity

$$\langle x \rangle = \int_0^\infty x p(x, Y) dx = \sqrt{\frac{2}{\pi}} \sigma e^{\lambda Y}. \quad (\text{B9})$$

On the other hand, if $w(x) = v(x)$ we get stationary solution $p(x, Y) = p(x, 0)$ that leads to constant

$$\langle x \rangle = \sqrt{\frac{2}{\pi}} \sigma. \quad (\text{B10})$$

Recall that discrete stationary solution of the general equation (24) is given by [75]

$$p_n(Y) = \frac{N^n}{n!} e^{-N}, \quad \langle n \rangle = N = 1/\alpha_s^2, \quad (\text{B11})$$

and matches the continuum intuitions above.

Appendix C: Additional plots

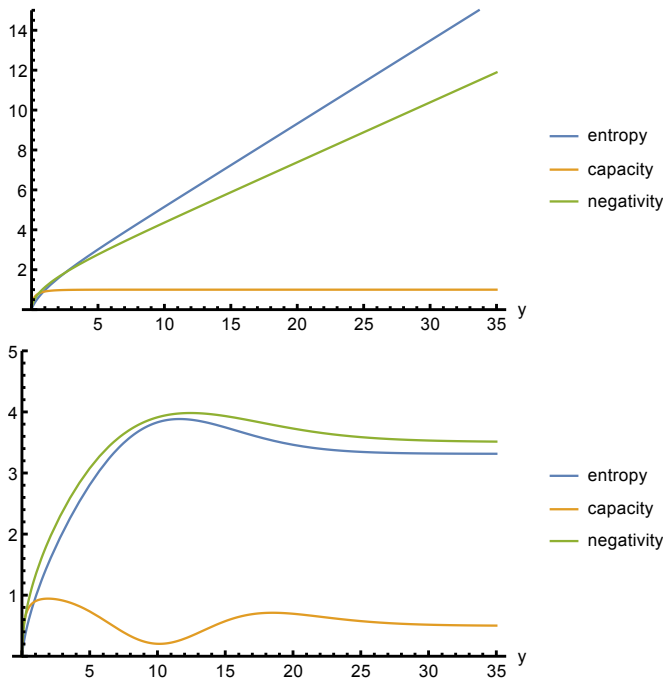


FIG. 5. Plot of entropy, capacity of entanglement and negativity extracted from solutions of eq. (2) and (24).

In this appendix we provide additional figures in linear scale that supplement those from the main body of the paper. In particular, for the two QCD models of the main text, together with entanglement entropy and capacity of entanglement we also evaluate the logarithmic negativity defined as [79]

$$\mathcal{N}(Y) = 2 \ln \left(\sum_n \sqrt{p_n(Y)} \right). \quad (\text{C1})$$

Clearly, the maximum and decrease of the entanglement entropy is now also visible in the evolution of the capacity of entanglement. The logarithmic negativity is positive meaning that the entropy is entanglement entropy i.e. quantum entropy.